Hittite Journal of Science and Engineering, 2020, 7 (2) 89-97
ISSN NUMBER: 2148-4171
DOI: 10.17350/HJSE19030000177

Gold Nanoparticles/Graphene Oxide Based Disposable Sensor System for Voltammetric Detection of Ceftizoxime

Gulcin Bolat[1] Yesim Tugce Yaman[1,2] Ceren Yardimci[3] and Serdar Abaci[1,2]
[1]Hacettepe University, Department of Chemistry, Ankara, Turkey
[2]Hacettepe University, Advanced Technologies Application and Research Center, Ankara, Turkey
[3]Hacettepe University, Department of Analytical Chemistry, Ankara, Turkey

ABSTRACT

In this study, gold nanoparticles (AuNPs) were deposited onto graphene oxide (GO) modified pencil graphite electrode (PGE) in order to construct a disposable sensor platform for the electrochemical detection of ceftizoxime (CFX). Initially, electrode surface was covered with GO by physical adsorption and then AuNPs were deposited on the surface by electro-deposition method. Morphological feature of the developed sensor was investigated by scanning electron microscope. The parameters effecting the experimental conditions such as adsorption time of graphene oxide, deposition time of gold nanoparticles, supporting electrolyte pH, pre-concentrating potential/time were optimized. Under optimum experimental conditions, good linearity was obtained for CFX response in the range between 0.02-2.0 µM of CFX concentrations with a low detection limit (0.442 nM) by stripping voltammetry. The AuNPs/GO modified PGE was implemented to pharmaceutical samples with good recovery values. This study results proved that developed disposable sensor is a good alternative for the practical application of CFX analysis.

Article History:
Received: 2019/10/30
Accepted: 2020/05/01
Online: 2020/06/26

***Correspondence to**: Serdar Abaci, Hacettepe University, Department of Chemistry, Ankara, Turkey*
E-Mail: sabaci@hacettepe.edu.tr
Phone: +90 (312) 297 6080
Fax: +90 (312) 299 2163

Keywords:
Gold nanoparticles; Graphene oxide; Cephalosporins; Ceftizoxime; Anodic stripping voltammetry.

INTRODUCTION

Cephalosporins are β-lactam antibiotics which their main core is formed by cephem derivative of 7-amino-cephalosporanic acid [1]. Due to their similar antimicrobial indications with penicillin's, this group of antibiotics are widely used in treatment for penicillin resistive bacteria. Further, they have been prescribed safely for penicillin allergic patients. Cephalosporins show bactericide effect against various microbial organisms-bacteria and they have been classified into generations depending on their spectrum of activity. Specifically, ceftizoxime sodium (CFX), belonging to third generation of semi-synthetic cephalosporins, has broad-spectrum resistance against β-lactamases [2] (Fig. 1). The most important features of third-generation cephalosporins (except Cefoperazone) includes the increased efficiency to gram-negative bacteria, high stability against hydrolysis by β-lactamases and in particular, being free of serious side effects in patients. Furthermore, some of them are known to overcome the blood-brain barrier [3]. CFX shows high antibacterial effect against a broad range of gram positive and negative bacteria such as *Staphylococcus pneumoniae, Haemophilusinfluenzae, Escherichia coli*, and *Neisseria gonorrhoeae* by penetrating into bacterial cell wall and consequently leading to effective destruction of bacteria [4]. CFX, with a relatively long elimination half-life (3-4 h), is administered through the oral route for the treatment of moderate bacterial infections [5]. It is active against putrefaction and clinically effective in eradicating bacteria causing urinary tract infections, acute pharyngitis, otitis media, tonsillitis, gonorrhea and pneumonia [3]. Given it's pharmacological significance and extended use, quantitative analysis of CFX in biological fluids has great clinical value in order to reveal biochemical processes that occur in the drug metabolism and also in pharmaceutical formulations to assure drug quality.

Up to now, analysis of CFX in various matrixes, such as human and animals, biological materials, food, waters and pharmaceuticals have been studied by several chromatographic and spectrometric methods [6–10]. Although they provide very efficient analyses for the sensitive detection of CFX, these methods have some handicaps such as high cost instrumentation, long

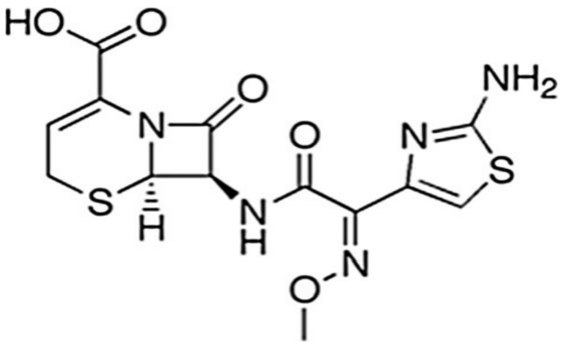

Figure 1. Chemical structure of Ceftizoxime.

analysis time, including the need for specialized staff. Since CFX is an electroactive molecule, electrochemistry is a promising approach for the analysis of CFX due to its benefits such as being simple, sensitive, fast and requiring portable and low-cost systems as well as being suitable for on-site detection. Up to now, only a few studies on the oxidation behavior and detection of CFX have been reported based on different electrochemical methodologies using solid electrodes. Jain et al., offered a fullerene based glassy carbon electrode (GCE) for the reduction of CFX in solubilized system and applied for the pharmaceutical tablet samples [11]. In another study, silver nanoparticle with nano graphite-diamond modified GCE was developed to determine the CFX in blood serum and commercial pharmaceutical tablet [12]. Nickel particle decorated on Poly(o-anisidine) sensor platform was constructed to detect CFX by Ojani et al. [13]. On the other hand, single-use sensor technologies offer some considerable advantages to design sensor platforms. Specifically, pencil graphite electrode (PGE), as a carbon based electrode, have extensively been applied in electroanalysis due to its benefits such as commercial availability, good electrochemical reactivity and mechanical resistance, feasibility for modification, as well as enabling disposable manipulation which eliminates the need for electrode surface cleaning steps [14]. Functionalization of the electrode surfaces with nanomaterials is crucial in order to significantly improve the electrochemical response. Standing out as an advanced material, graphene is a suitable nanomaterial for the electrochemical analysis due to its high electrical conductivity, high surface area, low cost and biocompatibility [15]. Graphene oxide (GO) is a valuable derivative of graphene which contains oxygen functional groups as distinct from the graphene [16]. Due to the outstanding features of GO, it has been extensively employed for the electrochemical determination of different analytes such as heavy metals [17], pathogens [18], pollutants [19] and drugs [20] etc. Metal nanoparticles have been used as a functional nanomaterial for the modification of electrochemical sensor surfaces. Especially, gold nanoparticle (AuNP) modified sensors are remarkably important surfaces owing to their excellent conductivity, high surface area and biocompatible properties [21]. To obtain highly electro-catalytic surfaces, AuNP's combined with other nanomaterials have widely been used in various analyses and catalysis [22–25] applications.

Hence, in the present study, AuNPs combined with GO modified PGE was constructed for the stripping analysis of CFX. AuNP/GO modified PGE was considered as an attractive platform from the stand point of easy use, cheapness and simple modification. Owing to considerable synergy between the AuNP and GO, anodic oxidation signal of CFX increased remarkably. The electrode surfaces were examined microscopically to prove the success of the modification. The experimental parameters such as adsorption time of graphene oxide, deposition time of gold nanoparticles, supporting electrolyte pH, pre-concentrating potential and time were optimized. Anodic stripping voltammetry (SWASV) measurements of CFX demonstrated good linear response with a low limit of detection (LOD) as 0.442 nM. The practical use of the sensor system was tested for commercial pharmaceutical tablets by standard addition method. The proposed sensor system has offered a low detection limit with respect to other studies in literature and also other parameters were comparable with the literature data.

MATERIAL AND METHODS

Reagents and Materials

Ceftizoxime sodium, gold (III) chloride trihydrate and graphene oxide (GO) were provided from Sigma Aldrich and Nanograf, respectively. 0.5 M of $HAuClO_4$ was prepared in 0.5 M of H_2SO_4. Britton-Robinson (B-R) buffer solution (0.04 M) was prepared by mixture of boric acid, acetic acid and phosphoric acid which was applied as a supporting electrolyte. Stock solution of CFX (10^{-2} M) was prepared in double distilled water and stored at +4 °C. More diluted solutions were prepared daily.

Instruments

CV, EIS and SWASV were recorded by Gamry interface 1000 model potentiostat/galvanostat. AuNP/GO modified PGE served as a working electrode. Pencil leads were purchased from local store in Turkey (0.5 mm diameter, Tombow). An Ag/AgCl (3M KCl) electrode was used as the reference and a platinum wire as the counter electrode. The surface morphology of the developed sensor was characterized by Zeiss Evo 60 EP-SEM. Besides, the AuNP/GO modified graphite surfaces were characterized by Energy-dispersive X-ray spectroscopy (EDX, Tescan/Czech Republic).

Fabrication of AuNP/GO/PGE sensor

Firstly, 1 cm of pencil leads were immersed in graphene oxide (GO) solution for 30 minutes. Afterwards, the leads were soaked in double distilled water for 5 seconds to remove the excess of GO attached on the surface. The GO modified electrodes were allowed to dry for 5 min at room temperature. Potential controlled electrolysis was used at - 0.3 V (vs. Ag/AgCl) for the electro-deposition of AuNPs on GO/PGE in 0.5 M $HAuClO_4$ solution (in 0.5 M H_2SO_4). The optimum electro-deposition time was found as 100 seconds.

Preparation of Drug Samples

Five tablets of Cefizox® (400 mg CFX per tablet) were weighed and pulverized in a mortar. Then, an average of 1 tablet weight was taken from this powder and dissolved in 100 mL double distilled water by ultrasonication for 1 hour. Upon centrifugation at 5000 rpm for 5 min, the supernatant was diluted in double distilled water.

Analytical Procedure

Electrochemical characterizations were performed by CV (between -0.2 V and 0.6 V (vs. Ag/AgCl)) and EIS (in the frequency range of 0.01–100,000 Hz) in redox probe solution (0.5 mM $Fe(CN)_6^{3-/4-}$ prepared in 0.1 M KCl). The electrochemical determination of CFX was carried out in 10.0 mL cell and BR buffer (pH 2.5 as optimum pH) was used as the supporting electrolyte by CV at potential from 0.7 V to 1.1 V (vs. Ag/AgCl). Square wave anodic stripping voltammetry (SWASV) was recorded from 0.6 V to 1.0 V (vs. Ag/AgCl) after a pre-concentrating step of 300 seconds at 0.6 V (vs. Ag/AgCl) accumulation and deposition time, respectively. After this pre-concentration step, stirring was stopped and 15s was waited as a release time. The pulse amplitude 4 mV, pulse size 50 mV and frequency 50 Hz were used as parameters of SWASV. Before the all electrochemical measurements, supporting electrolyte was purged with the nitrogen gas for 5 minutes.

RESULTS AND DISCUSSION

Morphology and Electrochemical Characterization of AuNP/GO modified PGE

In order to reveal the gradual changes on the electrode after the modifications, surface morphology of bare and modified pencil graphite electrodes (PGEs) were investigated with scanning electron microscopy (SEM). Fig. 2.a showed that bare PGE surface displayed irregular graphite layers with highly rough structure, as expected. When graphene oxide (GO) was deposited onto PGE surface, it was observed that single or few-layers of GO nano-sheets with high amount of wrinkles due to GO sheets were entangled with each other (Fig. 2.b). The nanosized AuNPs which were deposited by potential control electrolysis, were in a form of spherical structure uniformly distributed over the bare electrode surface and over the GO layers, respectively (Fig. 2.c,d). The morphology of the AuNP/GO modified PGE showed more even structure.

As it was shown in Fig. 2.g-h, the main elements of GO including carbon, and oxygen were all observed in EDX spectrum as expected [26]. Also, the presence of gold which resulted from the AuNPs on the surface of GO/PGE was confirmed with EDX analysis (Fig. 2.h). The carbon and oxygen peaks were observed on the bare graphite surface in Fig. 2.e-f. These results clearly suggested that AuNP/GO were successfully coated on the graphite surface.

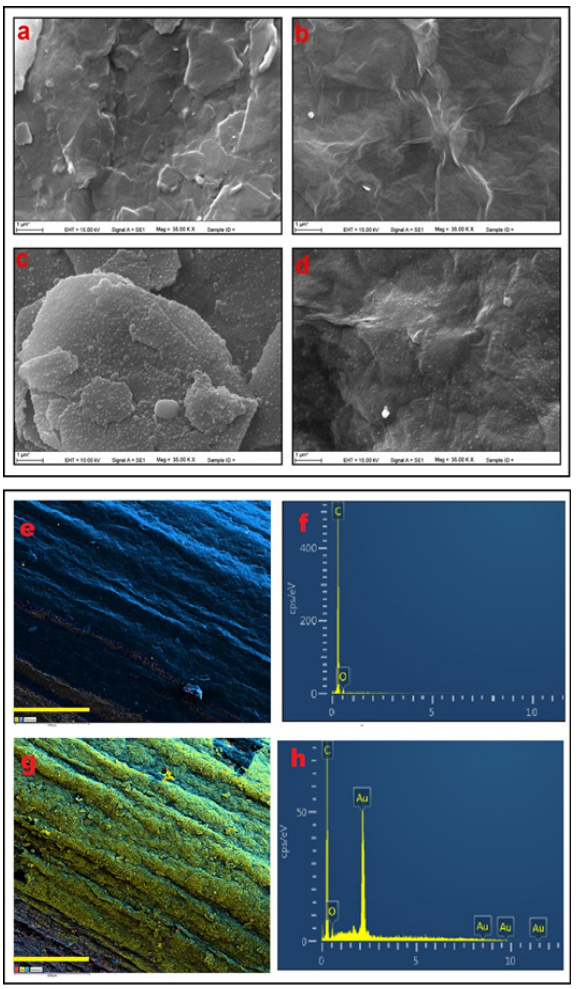

Figure 2. The scanning electron micrographs of **a)** Bare PGE, **b)** GO modified PGE, **c)** AuNP modified PGE, **d)** AuNP/GO modified PGE (Scale bar: 1 µm). EDX mapping of **e)** PGE (The colors: Blue:C; Yellow:O) and **g)** AuNP/GO/PGE (scale bar: 100 µm. The colors: Red:O; Blue:C; Yellow: Au) and corresponding elementel compositions of **f)** PGE and **h)** AuNP/GO/PGE.

Table 1. Anodic/cathodic peak currents (Ipa/Ipc) and peak potentials (Epa/Epc) at bare, GO modified and AuNP/GO modified PGEs.

Electrode	Ipa (µA)	Ipc (µA)	Epa (V)	Epc (V)	ΔEp (V)
PGE	336.0	323.0	0.306	0.173	0.133
GO/PGE	288.2	268.8	0.343	0.166	0.177
AuNP/GO/ PGE	461.7	468.6	0.292	0.175	0.117

To investigate the electrochemical behaviour of developed disposable nanosensor platform, cyclic voltammetry and impedance spectroscopy were employed in redox probe solution. Fig. 3.A depicts the decrease in anodic/cathodic peak currents of redox pairs at GO/PGE compared to bare PGE (Fig. 3.A.b and 2.A.a, respectively). Besides, peak-to-peak separation increased due to the negatively charged carboxyl groups of GO. When the medium pH is high enough, carboxyl groups in the GO structure are negatively charged and repel the negatively charged $Fe(CN)_6^{3-/4-}$ redox pair from the surface with electrostatic effects. Hence, the presence of GO on PGE impeded the electron transfer and reduced the peak currents [27]. When AuNP electrodeposition was performed onto GO film, AuNP/GO/PGE showed a well-defined CV, with approximately equal and reversible peaks (Fig. 3.A.c). The highest peak current values indicated a faster electron-transfer than the GO modified PGE. This was realized by the catalytic effect of AuNPs and increased

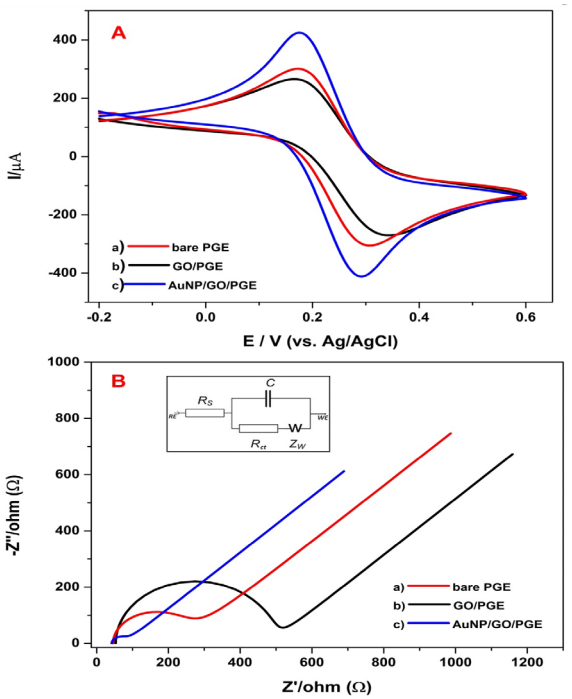

Figure 3. a) CVs showing a) bare, b) GO/PGE and c) AuNP/GO/PGE in 5 mM $Fe(CN)_6^{3-/4-}$ /0.1 M KCl at 50 mVs^{-1}. B) Nyquist diagrams of a) bare, b) GO/PGE and c) AuNP/GO/PGE in 5 mM $Fe(CN)_6^{3-/4-}$ /0.1 M KCl. (E: 0.2 V, Frequency: 100000-0.1 Hz). Inset: equivalent circuit for EIS spectrum. Rs: the electrolyte resistance, Cdl: double-layer capacitance, Rct: the electron transfer resistance, Zw: the Warburg impedance.

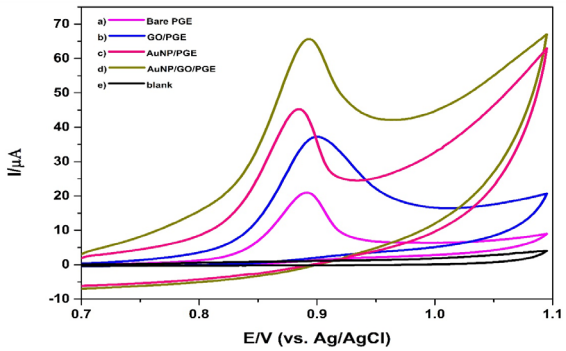

Figure 4. CVs for 50 µM of CFX in pH 3.0 B-R buffer solution at a) bare, b) GO modified, c) AuNP modified, d) AuNP/GO modified PGE. e) CV for AuNP/GO/PGE in the absence of CFX. (Scan rate: 100 mVs^{-1} vs. Ag/AgCl).

electrode surface area, accordingly. The corresponding results were summarized in Table 1.

To support this behavior of AuNP/GO/PGE, EIS method was utilized and obtained Nyquist diagrams were presented in Fig. 3.B. The charge transfer resistance (Rct) values were calculated from the obtained spectrum using Randles circuit at the electrode/solution interface (Fig. 3.B inset). The Rct values of bare and GO/PGE were calculated as 260 Ω and 440 Ω, respectively. The increased Rct can be explained by the restriction of electron transfer due to GO modification. The resistance of AuNP/GO modified electrode at the electrode/solution interface decreased, due to increased charge transfer, so, AuNP/GO/PGE had the lowest Rct (43 Ω) as expected. These results proved that modification of PGE surface was performed successfully.

The influence of modification of PGE on the electrochemical behavior CFX

The voltammetric response of CFX was examined at bare and modified surfaces (Fig. 4). All the CVs revealed an oxidation peak at about 0.9 V (vs. Ag/AgCl) and no reduction signal was recorded in the reverse scan due to irreversible nature of the electrode process for cephalosporins [28].

As previously reported, the oxidation of amino group at aminothiazole substituent to imino radical was responsible for the electrode process of this group of antibiotics [12] (Fig. 5).

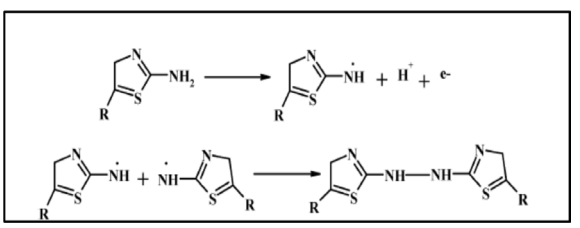

Figure 5. Electrochemical oxidation reactions of CFX.

As previously reported, the oxidation of amino group at aminothiazole substituent to imino radical was responsible for the electrode process of this group of antibiotics [12] (Fig. 5).

The recorded CVs for 50 µM of CFX in pH 3.0 B-R buffer showed that maximum peak current intensity was provided by GO/AuNP/PGE surface. The oxidation peak current was 3.5 times higher and the peak potential appeared at more negative potentials with respect to bare PGE. This can be ascribed to larger effective surface area and improved catalytic activity of the modified sensor surface. Thus, it was concluded that AuNP/GO modified PGE sensor system was suitable for sensitive CFX detection. In order to understand the effect of several experimental parameters, optimization studies were performed as below.

Effect of Scan Rate

The effect of scan rate was examined in the range of 10-400 mVs^{-1} at AuNP/GO/PGE (Fig. 6). The plot of oxidation peak current vs square root of scan rate showed excellent linearity. This linearity was given as follows (Eq1.)

$$I(\mu A) = 5.085\vartheta^{0.5} + 12.28 \qquad R^2 = 0.990 \qquad (1)$$

This behavior demonstrated that the electro-oxidation reaction of CFX was a typical diffusion controlled electrocatalytic process at AuNP/GO/PGE [11].

Effect of Electrolyte pH

The voltammetric behavior of CFX on the sensor was studied in BR buffer solutions of different pH values since the electrochemical characteristics is strongly dependent on the pH of the medium. Highest peak current was observed with the pH value of 2.5 and decreased up to pH value of 5.0 (Fig. 7). Thus, optimum pH value was determined as 2.5.

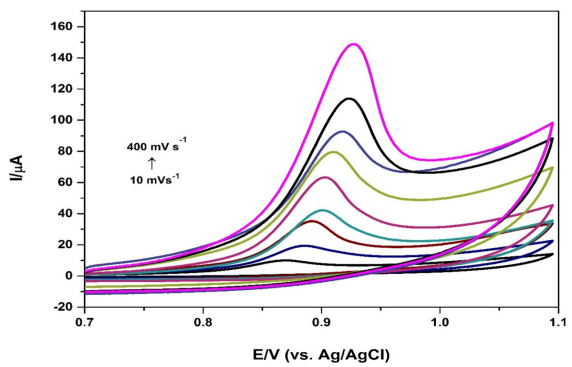

Figure 6. Scan rates from bottom to top: 10-400 mVs^{-1} for 50 µM CFX in pH 2.5 B-R Buffer.

Effect of AuNP and GO deposition time

After it was clearly demonstrated that the anodic oxidation of CFX increased when the modifying agents were combined together, AuNP/GO/PGE was employed in order to obtain improved electrochemical signal of the analyte. The dependence of response enhancement on GO and AuNP deposition time was examined. The physical adsorption time of GO was investigated between 15-90 minutes and the maximum oxidation peak current was obtained at 30 min (Fig. 8.a). After this adsorption time, peak current decreased which might have been due to electron transfer restriction with the increase of GO layer thickness. So, the optimum adsorption time of GO was used as 30 min.

After determining the optimization of physical adsorption time of GO, the bulk electrolysis time of AuNP onto GO/PGE was studied in the range of 25-300 s as deposition times (Fig. 8.b). The maximum peak current was obtained with deposition time of 100 s which promoted the electron transfer between the CFX and the electrode, and higher deposition times induced hinderance of the transfer. Therefore, 100 s of AuNP electrodeposition time was applied for further studies.

Effect of Pre-concentration Step

The pre-concentration of stripping analysis has two main steps; namely deposition potential and deposition time of the analyte. The deposition potential was changed at fixed concentration of CFX in the range of 0.0 to 0.7 V (vs. Ag/AgCl) at AuNP/GO modified PGE and stripping voltammograms were recorded. As shown in Fig. 9.a, according to the plot for applied deposition potential vs. the oxidation current of CFX, the measured peak current increased from 0.0 V to 0.6 V (vs. Ag/AgCl), and a roll-off rate was observed on the peak current after this value indicating that at more cathodic potentials which are close to oxidation potential of the analyte, CFX molecules are

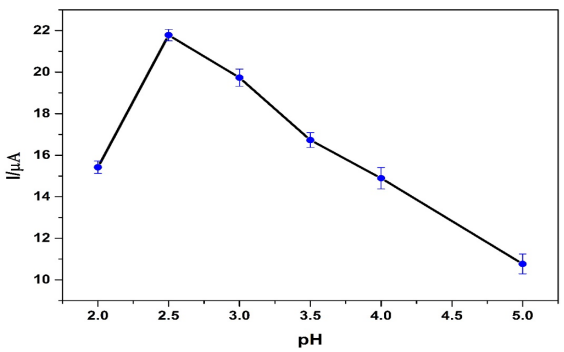

Figure 7. The current response of 5 µM CFX at AuNP/GO modified PGE at different pH (2.0, 2.5, 3.0, 3.5, 4.0, 5.0) BR buffer. Conditions: frequency: 15 Hz; step amplitude: 30 mV; pulse amplitude: 4 mV; $E_{deposition}$(E_{dep}): 0.5 V; tdeposititon (t_{dep}): 30 s.

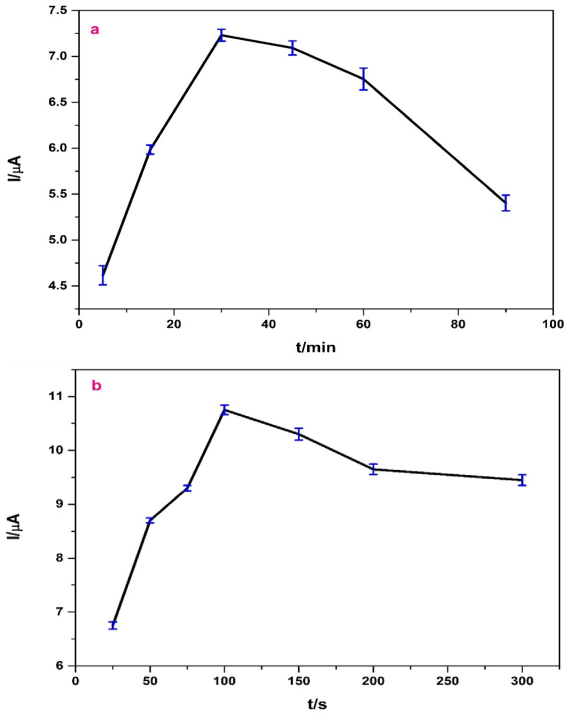

Figure 8. a) Effect of GO adsorption time onto PGE, b) Effect of electrodeposition time of AuNP to electrochemical response of 5 μM CFX. (Under the same SWASV experimental conditions).

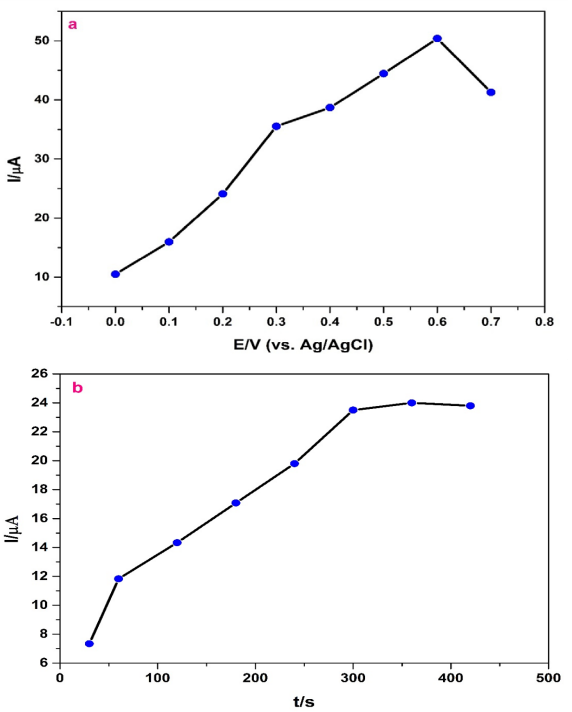

Figure 9. a) Effect of deposition potential and b) deposition time on the oxidation peak current of 0.5 μM CFX. (Under the same SWASV experimental conditions).

not strongly adsorbed on the electrode surface. Therefore, the optimum deposition potential was determined as 0.6 V (vs. Ag/AgCl).

To identify the optimum deposition time of CFX, different durations (60-420 s) at the optimum deposition potential were examined (Fig. 9.b). Up to 300 s, the peak currents increased and further increase in accumulation time yielded to almost stable response. This result proved that the sensor surface was saturated at 300 s deposition time. So, the optimum deposition time was selected as 300 s.

Analytical performance of the AuNP/GO/PGE

Since stripping analysis provides more sensitive measurements, it has frequently been applied for various drug determination studies [29–31]. Hence, under the optimized conditions, SWASV was performed for the quantitive detection of CFX (Fig. 10). The well-defined oxidation peak currents with respect to the increasing CFX concentrations were monitored and the measured peak currents increased linearly with CFX concentrations in the range of 0.02-2.0 μM. The corresponding calibration graph was illustrated in Fig. 10 (inset).

The obtained linear equation was (Eq.2),

$$I(\mu A) = 45.21\ C(\mu \mathrm{M}) + 3.412 \quad \mathrm{R}^2 = 0.9985\ . \qquad (2)$$

As a result, based on 3σ/m equation (σ is standard deviation of the analytical signal for the blank solution (n=3), m is the calibration curve slope), the LOD and LOQ were determined as 0.442 nM and 1.32 nM, respectively. When compared with other reported electrochemical studies about CFX (Table 2), the proposed sensing system had compatible results.

Furthermore, the intra/inter-day reproducibility of the AuNP/GO modified surface was examined by SWASV. To estimate reproducibility of the electrode, six AuNP/GO/PGE were fabricated independently and the RSD values for these electrodes were 2.43% (n=3) and 2.26% (for 6 days). The developed AuNP/GO/PGE showed good reproducible results. The interference study results showed

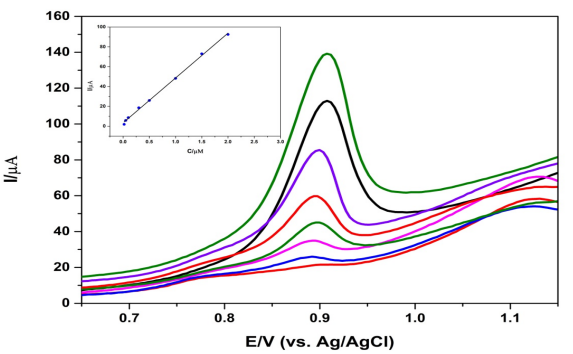

Figure 10. SWASV curves at AuNP-GO modified PGE in BRT containing 0.02; 0.05; 0.1; 0.5; 1.0; 1.50 and 2.00 μM (down to up) of CFX. (Inset: Linear calibration graph for CFX).

Table 2. List of electrochemical sensors of CFX.

Working electrode type	Method	LOD (M)	Linear Range (M)	Reference
AgNPs-ND-G/GCE	LSV	$6.0x10^{-9}$	2.0x10-8-7x10^{-6}	[12]
Fullerene/GCE	SWV	$6.6x10^{-10}$	2.96x10-6-25.4 x10^{-6}	[11]
Poly(o-anisidine)/SDS/Ni/CPE	chronoamperometry	$8.0x10^{-5}$	1.0x10-5-2.0x10^{-3}	[13]
MIP/Ag@AuNPs/ILs/GCE	DPV	$2.0x10^{-12}$	1.0x10-9-1.0x10^{-11}	[32]
HGNPs/rGO/PGE	AdDPV	$3.5x10^{-13}$	1.0x10-12-1.0x10^{-11} 1.0x10-11- 1.0x10^{-9}	[33]
AuNP/GO/PGE	SWASV	$4.42x10^{-10}$	2.0x10-8-2.0x10^{-6}	This work

GCE: Glassy carbon electrode, AgNPs-ND-G: silver nanoparticles Decorated Nano Diamond, SDS: sodium dodesulphate, CPE: carbon paste electrode, MIP/Ag@AuNPs/ILs: molecularly imprinted polymer based silver@gold nanoparticles/ionic liquid, HGNPs/rGO: Hollow gold nanoparticles/reduced graphene oxide, AdDPV: adsorptive differential pulse voltammetry.

that 250 fold concentration of ascorbic acid, 150 fold concentration of glucose and 150 fold concentration of lidocaine had no significant influence on the measured 0.5 µM CFX peak current (RSD values less than 5%).

Real Sample Analysis

The commercial CFX tablet was used to show the practical application of AuNP/GO modified PGE. The tablet samples were analysed by standard addition method and the recovery values of different concentrations of spiked CFX were given in Table 3.

The recovery and precision values confirmed that the adjuvants of the drug did not show important interference on the voltammetric response of CFX. These results clearly proved that this sensor system can be used in real samples for the detection of CFX with high accuracy.

CONCLUSION

A simple and an effective disposable sensor system based on AuNP/GO was developed for the electrochemical detection of CFX for the first time. When PGE surface was coated with AuNP/GO, the oxidation peak of CFX improved remarkably due to a synergistic effect. The optimum conditions were examined for the detection of CFX by SWASV. The described ultra-sensitive detection strategy had good sensing performance and exhibited comparable results with the literature. To demonstrate the success of the practical application, the developed sensor system was applied to the commercial CFX tablet and the obtained recovery values showed that the proposed system can be used in real matrixes with high accuracy. The disposable modified sensor offers favourable features for the electrochemical detection of CFX in terms of high sensitivity, rapidness, simplicity and cost-effectiveness.

Table 3. Determination of CFX in tablet samples by standard addition method (n=3).

Sample	Added (µM)	Detected (µM)	RSD (%)	Recovery (%)
Tablet	0.0264	0.0261	1.60	101
	0.0600	0.0581	1.39	97.0
	0.0750	0.0742	1.29	99.0

ACKNOWLEDGEMENT

The authors acknowledge to the Research Council of Hacettepe University for financially supporting this study (THD-2015-7394).

References

1. Abo El-Maali N, Ghandour M a., Kauffmann JM. Cephalosporin antibiotics at carbon paste and modified carbon paste electrodes in both aqueous and biological media. Bioelectrochemistry and Bioenergetics 38 (1995) 91–97. DOI: 10.1016/0302-4598(95)01822-V.
2. Facca B, Frame B, Triesenberg S. Population pharmacokinetics of ceftizoxime administered by continuous infusion in clinically ill adult patients. Antimicrobial Agents and Chemotherapy 42 (1998) 1783–1787.
3. Wiseman LR, Benfield P. Cefprozil: A Review of its Antibacterial Activity, Pharmacokinetic Properties, and Therapeutic Potential. Drugs 45 (1993) 295–317. DOI: 10.2165/00003495-199345020-00008.
4. Jain R, Gupta VK, Jadon N, Radhapyari K. Voltammetric determination of cefixime in pharmaceuticals and biological fluids. Analytical Biochemistry 407 (2010) 79–88. DOI: 10.1016/j.ab.2010.07.027.
5. Ferreira SMZMD, Domingos GP, Ferreira DDS, Rocha TGR, Serakides R, De Faria Rezende CM, et al. Technetium-99m-labeled

ceftizoxime loaded long-circulating and pH-sensitive liposomes used to identify osteomyelitis. Bioorganic and Medicinal Chemistry Letters 22 (2012) 4605–4608. DOI: 10.1016/j.bmcl.2012.05.105.

6. Sanli S, Sanli N, Gumustas M, Ozkan S a., Karadas N, Aboul-Enein HY. Simultaneous estimation of ceftazidime and ceftizoxime in pharmaceutical formulations by HPLC method. Chromatographia 74 (2011) 549–558. DOI: 10.1007/s10337-011-2116-1.
7. Moore CM, Sato K, Hattori H, Katsumata Y. Improved HPLC method for the determination of cephalosporins in human plasma and a new solid-phase extraction procedure for cefazolin and ceftizoxime. Clinica Chimica Acta 190 (1990) 121–123. DOI: 10.1016/0009-8981(90)90290-9.
8. Péhourcq F, Jarry C. Determination of third-generation cephalosporins by high-performance liquid chromatography in connection with pharmacokinetic studies. Journal of Chromatography A 812 (1998) 159–178. DOI: 10.1016/S0021-9673(98)00265-9.
9. Wang L, Zheng X, Zhong W, Chen J, Jiang J, Hu P. Validation and Application of an LC–MS-MS Method for the Determination of Ceftizoxime in Human Serum and Urine. Journal of Chromatographic Science 54 (2016) 713–719. DOI: 10.1093/chromsci/bmv243.
10. Al-Momani I. Spectrophotometric determination of selected cephalosporins in drug formulations using flow injection analysis. Journal of Pharmaceutical and Biomedical Analysis 25 (2001) 751–757. DOI: 10.1016/S0731-7085(01)00368-5.
11. Jain R, Rather JA, Dwivedi A, Vikas. Highly Sensitive and Selective Voltammetric Sensor Fullerene Modified Glassy Carbon Electrode for Determination of Cefitizoxime in Solubilized System. Electroanalysis 22 (2010) 2600–2606. DOI: 10.1002/elan.201000243.
12. Shahrokhian S, Ranjbar, S, Ghalkhani, M.. Modification of the Electrode Surface by Ag Nanoparticles Decorated Nano Diamond-graphite for Voltammetric Determination of Ceftizoxime. Electroanalysis, 28, (2016) 469-476. DOI: 10.1002/elan.201500377
13. Ojani R, Raoof JB, Zamani S. A novel sensor for cephalosporins based on electrocatalytic oxidation by poly(o-anisidine)/SDS/Ni modified carbon paste electrode. Talanta 81 (2010) 1522–1528. DOI: 10.1016/j.talanta.2010.02.062.
14. Erdem A, Papakonstantinou P, Murphy H. Direct DNA hybridization at disposable graphite electrodes modified with carbon nanotubes. Analytical Chemistry 78 (2006) 6656–6659. DOI: 10.1021/ac060202z.
15. Pumera M, Ambrosi A, Bonanni A, Chng ELK, Poh HL. Graphene for electrochemical sensing and biosensing. TrAC-Trends in Analytical Chemistry 29 (2010) 954–965. DOI: 10.1016/j.trac.2010.05.011.
16. Yuan B, Xu C, Deng D, Xing Y, Liu L, Pang H, et al. Graphene oxide/nickel oxide modified glassy carbon electrode for supercapacitor and nonenzymatic glucose sensor. Electrochimica Acta 88 (2013) 708–712. DOI: 10.1016/j.electacta.2012.10.102.
17. Promphet N, Rattanarat P, Rangkupan R, Chailapakul O, Rodthongkum N. An electrochemical sensor based on graphene/polyaniline/polystyrene nanoporous fibers modified electrode for simultaneous determination of lead and cadmium. Sensors and Actuators B: Chemical 207 (2015) 526–534. DOI: 10.1016/j.snb.2014.10.126.
18. Tiwari I, Singh M, Pandey CM, Sumana G. Electrochemical genosensor based on graphene oxide modified iron oxide-chitosan hybrid nanocomposite for pathogen detection. Sensors and Actuators, B: Chemical 206 (2015) 276–283. DOI: 10.1016/j.snb.2014.09.056.
19. Gan T, Sun J, Huang K, Song L, Li Y. A graphene oxide-mesoporous MnO2 nanocomposite modified glassy carbon electrode as a novel and efficient voltammetric sensor for simultaneous determination of hydroquinone and catechol. Sensors and Actuators, B: Chemical 177 (2013) 412–418. DOI: 10.1016/j.snb.2012.11.033.
20. Cheemalapati S, Palanisamy S, Mani V, Chen SM. Simultaneous electrochemical determination of dopamine and paracetamol on multiwalled carbon nanotubes/graphene oxide nanocomposite-modified glassy carbon electrode. Talanta 117 (2013) 297–304. DOI: 10.1016/j.talanta.2013.08.041.
21. Yaman YT, Abaci S. Sensitive adsorptive voltammetric method for determination of Bisphenol A by gold nanoparticle/polyvinylpyrrolidone-modified pencil graphite electrode. Sensors (Switzerland) 16 (2016) 756. DOI: 10.3390/s16060756.
22. Suea-Ngam A, Rattanarat P, Wongravee K, Chailapakul O, Srisa-Art M. Droplet-based glucosamine sensor using gold nanoparticles and polyaniline-modified electrode. Talanta 158 (2016) 134–141. DOI: 10.1016/j.talanta.2016.05.052.
23. Afkhami A, Bahiraei A, Madrakian T. Gold nanoparticle/multi-walled carbon nanotube modified glassy carbon electrode as a sensitive voltammetric sensor for the determination of diclofenac sodium. Materials Science and Engineering C 59 (2016) 168–176. DOI: 10.1016/j.msec.2015.09.097.
24. Saengsookwaow C, Rangkupan R, Chailapakul O, Rodthongkum N. Nitrogen-doped graphene-polyvinylpyrrolidone/gold nanoparticles modified electrode as a novel hydrazine sensor. Sensors and Actuators, B: Chemical 227 (2016) 524–532. DOI: 10.1016/j.snb.2015.12.091.
25. Kanyong P, Rawlinson S, Davis J. Gold nanoparticle modified screen-printed carbon arrays for the simultaneous electrochemical analysis of lead and copper in tap water. Microchimica Acta 183 2016 2361–2368. DOI: 10.1007/s00604-016-1879-3.
26. Mani V, Periasamy A P, Chen S. Highly selective amperometric nitrite sensor based on chemically reduced graphene oxide modified electrode. Electrochemistry Communications 17 2012 75-78. DOI: 10.1016/j.elecom.2012.02.009
27. Yavuz S, Erkal A, Af İ, Solak AO. Carbonaceous Materials-12 : a Novel Highly Sensitive Graphene Oxide-Based Carbon Electrode : Preparation , Characterization and Heavy Metal Analysis in Food Samples 9 (2016) 322-331. DOI: 10.1007/s12161-015-0198-3.
28. Sleegers N, Van Nuijs ALN, Van Den Berg M, De Wael K. Cephalosporin Antibiotics: Electrochemical Fingerprints and Core Structure Reactions Investigated by LC-MS/MS. Analytical Chemistry 91 (2019) 2035–2041. DOI: 10.1021/acs.analchem.8b04487.
29. Rodríguez J, Castañeda G, Lizcano I. Electrochemical sensor for leukemia drug imatinib determination in urine by adsorptive striping square wave voltammetry using modified screen-printed electrodes. Electrochimica Acta 269 (2018) 668–675. DOI: 10.1016/j.electacta.2018.03.051.
30. Santos AM, Wong A, Cincotto FH, Moraes FC, Fatibello-Filho O. Square-wave adsorptive anodic stripping voltammetric determination of norfloxacin using a glassy carbon electrode modified with carbon black and CdTe quantum dots in a chitosan film. Microchimica Acta 186 (2019) 148. DOI: 10.1007/s00604-019-3268-1.
31. Temerk YM, Ibrahim HSM, Schuhmann W. Square Wave Cathodic Adsorptive Stripping Voltammetric Determination of the Anticancer Drugs Flutamide and Irinotecan in Biological Fluids Using Renewable Pencil Graphite Electrodes 28 (2016) 372–379. DOI: 10.1002/elan.201500329.
32. Beytur M, Kardaş F, Akyıldırım O, Özkan A, Bankoğlu B, Yüksek H, et al. PT. Journal of Molecular Liquids 251 (2017) 212-217. DOI:

10.1016/j.molliq.2017.12.060.
33. Azadmehr F, Zarei K. Ultrasensitive determination of ceftizoxime using pencil graphite electrode modified by hollow gold nanoparticles / reduced graphene oxide. Arabian Journal of Chemistry 2018, (in press). DOI: 10.1016/j.arabjc.2018.02.004.